Published OnlineFirst April 3, 2007; DOI: 10.1158/1535-7163.MCT-06-0477



# Activation of a novel ataxia-telangiectasia mutated and Rad3 related/checkpoint kinase 1–dependent prometaphase checkpoint in cancer cells by diallyl trisulfide, a promising cancer chemopreventive constituent of processed garlic

**Anna Herman-Antosiewicz, Silvia D. Stan, Eun-Ryeong Hahm, Dong Xiao, and Shivendra V. Singh**

**Department of Pharmacology and University of Pittsburgh Cancer Institute, University of Pittsburgh School of Medicine, Pittsburgh, Pennsylvania**

## Abstract

**Diallyl trisulfide (DATS), a cancer chemopreventive constituent of garlic, inhibits growth of cancer cells by interfering with cell cycle progression, but the mechanism is not fully understood. Here, we show the existence of a novel ataxia-telangiectasia mutated and Rad3 related (ATR)/checkpoint kinase 1 (Chk1)–dependent checkpoint partially responsible for DATS-mediated prometaphase arrest in cancer cells, which is different from the recently described γ irradiation–induced mitotic exit checkpoint. The PC-3 human prostate cancer cells synchronized in prometaphase by nocodazole treatment and released to DATS-containing medium remained arrested in prometaphase, whereas the cells released to normal medium exited mitosis and resumed cell cycle. The mitotic arrest was maintained even after 4 h of culture of DATS-treated cells (4-h treatment) in drug-free medium. The DATS-arrested mitotic cells exhibited accumulation of anaphase-promoting complex/cyclosome (APC/C) substrates cyclin A and cyclin B1 and hyperphosphorylation of securin, which was accompanied by increased phosphorylation of the APC/C regulatory subunits Cdc20 and Cdh1. The DATS-mediated accumulation of cyclin B1 and hyperphosphorylation of securin, Cdc20, and Cdh1 were partially but markedly attenuated by knockdown of Chk1 or ATR protein. The U2OS osteosarcoma cells expressing doxycycline-inducible kinase dead ATR were significantly more resistant not only to DATS-mediated prometaphase arrest but also to the accumulation of cyclin B1 and hyperphosphorylation of securin, Cdc20, and Cdh1 compared with cells expressing wild-type ATR. However, securin protein knockdown failed to rescue cells from DATS-induced prometaphase arrest. In conclusion, the present study describes a novel signaling pathway involving ATR/Chk1 in the regulation of DATS-induced prometaphase arrest. [Mol Cancer Ther 2007;6(4):1249–61]**

## Introduction

Epidemiologic studies continue to support the premise that dietary intake of *Allium* vegetables such as garlic may be protective against the risk of various types of malignancies, including cancer of the prostate (1–4). Anticarcinogenic effect of *Allium* vegetables is attributed to organosulfur compounds (OSC), which are released upon processing (e.g., cutting or chewing) of these vegetables (5). *Allium* vegetable-derived OSCs, including diallyl sulfide (DAS), diallyl disulfide (DADS), and/or diallyl trisulfide (DATS), have been shown to inhibit cancer in animal models induced by a variety of carcinogens including tobacco-derived chemicals (6–10). For instance, naturally occurring OSC analogues are highly effective in affording protection against benzo(*a*)pyrene-induced forestomach and pulmonary carcinogenesis in mice (7), *N*-nitrosomethylbenzylamine–induced esophageal cancer in rats (8), azoxymethane-induced colon carcinogenesis in rats (9), and *N*-methyl-*N*-nitrosourea–induced rat mammary carcinogenesis (10). The OSCs are believed to inhibit chemically induced cancers by increasing the expression of phase 2 carcinogen-detoxifying enzymes, including glutathione transferases and quinone reductase and/or by inhibiting cytochrome P450–dependent monooxygenases (11–13). We have also shown previously that p.o. administration of DADS and DATS significantly inhibit growth of H-*ras* oncogene transformed and PC-3 human prostate cancer xenografts in nude mice, respectively, without causing weight loss or any other side effects (14, 15).

More recent studies have revealed that certain naturally occurring OSC analogues can inhibit growth of cultured cancer cells by causing $G_2$-M phase cell cycle arrest and apoptosis induction (16–26). In addition, DATS inhibits angiogenic features of human umbilical vein endothelial

Received 8/9/06; revised 1/24/07; accepted 2/26/07.

**Grant support:** U.S. Public Health Service grants CA113363 and CA115498, awarded by the National Cancer Institute.

The costs of publication of this article were defrayed in part by the payment of page charges. This article must therefore be hereby marked *advertisement* in accordance with 18 U.S.C. Section 1734 solely to indicate this fact.

**Note:** Current address for A. Herman-Antosiewicz: Department of Molecular Biology, University of Gdańsk, Kladki 24, 80-822 Gdansk, Poland.

**Requests for reprints:** Shivendra V. Singh, Department of Pharmacology, University of Pittsburgh Cancer Institute, Hillman Cancer Center Research Pavilion, 2.32A, 5117 Centre Avenue, Pittsburgh, PA 15213. Phone: 412-623-3263; Fax: 412-623-7828. E-mail: singhs@upmc.edu



doi:10.1158/1535-7163.MCT-06-0477

Published OnlineFirst April 3, 2007; DOI: 10.1158/1535-7163.MCT-06-0477



cells *in vitro* (27). An understanding of the mechanism by which OSCs cause apoptosis and cell cycle arrest is critical for their further development as clinically useful anticancer agents because this knowledge could facilitate identification of mechanism-based biomarkers potentially useful in future clinical trials. Significant progress has been made toward our understanding of the signaling pathways leading to OSC-induced apoptosis. For example, the DADS-induced apoptosis in human colon cancer cells correlates with an increase in the level of intracellular calcium (16). In MDA-MB-231 human breast cancer cell line, the DADS-induced apoptosis is associated with induction of Bax protein, down-regulation of Bcl-xL protein expression, and activation of caspase-3 (17). Using PC-3 and DU145 human prostate cancer cells as a model, we have shown that the DATS-induced cell death is caused by c-Jun $NH_2$-terminal kinase and extracellular signal-regulated kinase–mediated phosphorylation of Bcl-2 and inhibition of Akt kinase (21, 25). Despite these advances, however, the mechanism by which DATS causes cell cycle arrest is not fully defined.

Recently, we investigated the mechanism of DATS-induced cell cycle arrest using PC-3 and DU145 cells as a model (22, 24). We found that the DATS-treated cells are arrested in both $G_2$ phase and mitosis (22, 24). The DATS-induced $G_2$ phase cell cycle arrest correlates with reactive oxygen species (ROS)–dependent destruction and $Ser^{216}$ phosphorylation of Cdc25C, leading to the inhibition of cyclin-dependent kinase 1 (Cdk1; ref. 22). The DATS-mediated ROS generation is caused by an increase in labile iron due to increased degradation of iron storage protein ferritin (26). Interestingly, we also found that the DATS-induced mitotic arrest is significantly attenuated by knockdown of DNA damage checkpoint intermediary checkpoint kinase 1 (Chk1; ref. 24). Despite these advances, the mechanism by which Chk1 regulates DATS-induced mitotic arrest remains elusive. The present study indicates that DATS treatment causes prometaphase arrest in cancer cells due to the inactivation of anaphase-promoting complex/cyclosome (APC/C), which is partially dependent on ataxia-telangiectasia mutated and Rad3 related (ATR)/Chk1 activation.

## Materials and Methods

### Reagents

DATS was purchased from LKT Laboratories (St. Paul, MN). OligofectAMINE was from Invitrogen (Carlsbad, CA), G418, tissue culture media, penicillin/streptomycin antibiotic mixture, and fetal bovine serum (FBS) were from Life Technologies (Grand Island, NY), propidium iodide, nocodazole, 4′,6-diamidino-2-phenylindole (DAPI), and phosphatase inhibitors were from Sigma (St. Louis, MO), RNase A was from Promega (Madison, WI), doxycycline was from Clontech (Palo Alto, CA), λ protein phosphatase was from New England Biolabs (Beverly, MA), and protease inhibitor cocktail was from BD PharMingen (San Diego, CA). The antibodies against cyclin B1, cyclin A, Cdc20, Cdc27 and ATR, and protein A agarose beads were from Santa Cruz Biotechnology (Santa Cruz, CA); the antibodies against Chk1 and phospho-($Ser^{317}$)-Chk1 were from Cell Signaling Technology (Beverly, MA); an antibody against securin was from MBL (Woburn, MA); anti-Cdh1 antibody was from NeoMarkers (Fremont, CA); anti–α-tubulin and anti-Flag antibodies were from Sigma; and antibody specific for the detection of phospho-($Ser^{10}$)-histone H3 was from Upstate Biotechnology (Lake Placid, NY); anti-actin antibody was from Oncogene Research Products (San Diego, CA), and FITC-conjugated goat anti-rabbit immunoglobulin G was from Jackson Immunoresearch (West Grove, PA).

### Cell Culture and Cell Synchronization

Monolayer cultures of PC-3 cells were maintained in F-12K Nutrient Mixture (Kaighn's modification) supplemented with 7% (v/v) non–heat-inactivated FBS and antibiotics. The PC-3 cells were synchronized in prometaphase stage by a 24-h treatment with 0.1 μg/mL nocodazole. Subsequently, the cells were collected by mechanical shaking, washed with PBS, and plated in fresh medium containing either DMSO or 40 μmol/L DATS. Stock solution of DATS was prepared in DMSO, and an equal volume of DMSO was added to controls (final concentration, 0.2%). The DU145 cultures were maintained in Eagle's MEM supplemented with 1 mmol/L sodium pyruvate, 0.1 mmol/L non–essential amino acids, 1.5 g/L sodium bicarbonate, 10% (v/v) non–heat-inactivated FBS, and antibiotics. Osteosarcoma U2OS cells with doxycycline-inducible expression of either wild-type ATR or a dominant negative ATR mutant, a generous gift from Dr. P. Nghiem (Dana-Farber Cancer Institute, Boston, MA), were cultured in McCoy's 5A modified medium supplemented with 10% FBS (Tet system approved; Clontech, Palo Alto, CA), 400 μg/mL G418, and 200 μg/mL hygromycin (28). Expression of Flag-tagged wild-type ATR or kinase dead ATR was induced by treatment with 1 μg/mL doxycycline for 48 h. Each cell line was maintained at 37°C in an atmosphere of 5% $CO_2$ and 95% air.

### Analysis of Cell Cycle Distribution

Cell cycle distribution in control (DMSO-treated) and DATS-treated PC-3 cells was determined by flow cytometry following staining with propidium iodide as we described previously (22, 24). Briefly, cells ($5 \times 10^5$) were plated, allowed to attach by overnight incubation, and exposed to DMSO (control) or desired concentration of DATS for specified time periods. Both floating and adherent cells were collected, washed with PBS, fixed with 70% ethanol, and incubated for 30 min at room temperature with propidium iodide and RNase A (22, 24). Stained cells were analyzed using a Coulter Epics XL Flow Cytometer (Miami, FL). Cells in different phases of the cell cycle were computed for control and DATS-treated cultures.

### Immunoblotting

Cells were treated with DATS as described above and lysed as we described previously (24). The lysate was cleared by centrifugation at 14,000 rpm for 15 min. Lysate proteins were resolved by SDS-PAGE and transferred onto

Published OnlineFirst April 3, 2007; DOI: 10.1158/1535-7163.MCT-06-0477



polyvinylidene difluoride membrane. The membrane was treated with a solution containing 10 mmol/L Tris (pH 7.4), 150 mmol/L NaCl, 0.05% Tween 20, and 5% nonfat dry milk and incubated with the desired primary antibody for 1 to 2 h at room temperature or overnight at 4°C. The membrane was treated with appropriate secondary antibody for 1 h at room temperature. The immunoreactive bands were visualized by enhanced chemiluminescence method. The blots were stripped and reprobed with anti-actin or anti–α-tubulin antibody to normalize for differences in protein loading. To quantify changes in protein levels, the intensity of the immunoreactive bands was determined by densitometric scanning and corrected for loading control.

### RNA Interference

RNA interference of Chk1 was done using small interfering RNA (siRNA) duplexes (GCG UGC CGU AGA CUG UCC AdTdT) from Dharmacon (Lafayette, CO). The securin-specific siRNA 1 (sequence not revealed by the manufacturer) and a control nonspecific siRNA (UUC UCC GAA CGU GUC ACG UdTdT) were purchased from Qiagen (Valencia, CA). The securin-specific siRNA 2, which is a pool of three target-specific 20- to 25-nt siRNA, was purchased from Santa Cruz Biotechnology. The ATR-targeted siRNA (GAC GGU GUG CUC AUG CGG CdTdT) was obtained from Qiagen. For transfection, cells were plated in six-well plates, allowed to attach, and transfected at 30% confluency with siRNA (200 nmol/L for Chk1 siRNA, 25 nmol/L for securin siRNA 1, and 100 nmol/L for securin siRNA 2 and ATR siRNA) using OligofectAMINE according to the manufacturer's recommendations. After 24 h, cells were treated with DATS or DMSO (control) for the specified time period. Both floating and adherent cells were collected and processed for flow-cytometric analysis of histone H3 phosphorylation or immunoblotting of different proteins.

### Microscopic Analysis of Mitotic Cells

The mitotic cells were analyzed by fluorescence microscopy after staining with anti–α-tubulin antibody and/or DAPI. Briefly, desired cells ($2 \times 10^5$) were grown on coverslips and allowed to attach by overnight incubation at 37°C. The cells were then exposed to DMSO or the indicated concentration of DATS for specified time period at 37°C, washed with PBS, and fixed at 4°C overnight using 2% paraformaldehyde. Subsequently, the cells were permeabilized with 0.1% Triton X-100 for 15 min at room temperature, washed with PBS, and blocked with PBS containing 0.5% (w/v) bovine serum albumin (BSA) and 0.15% (w/v) glycine (BSA buffer) for 1 h at room temperature. Cells were treated with anti–α-tubulin antibody (1:4,000 dilution in BSA buffer) for 1 h at room temperature. Cells were then washed with BSA buffer and incubated with 1 μg/mL Alexa Fluor 568–conjugated goat anti-mouse antibody (Molecular Probes, Eugene, OR) for 1 h at room temperature followed by counterstaining with DAPI. In some experiments, control (DMSO-treated) and DATS-treated cells were stained with DAPI alone. Slides were mounted, and mitotic figures or multinucleated cells were examined under a Leica DM IRB fluorescence microscope.

### λ Protein Phosphatase Treatment

The λ protein phosphatase treatment was done according to the protocol provided by the manufacturer (New England Biolabs). Briefly, 60 μg of protein from lysates of cells treated for 8 h with 40 μmol/L DATS or DMSO were incubated with either λ protein phosphatase (400 units) or the control buffer at 30°C for 4 h. The samples were used for the immunoblotting of securin.

### Flow Cytometric Analysis of $Ser^{10}$ Phosphorylated Histone H3

The effect of DATS treatment on $Ser^{10}$ phosphorylation of histone H3, a sensitive marker for mitotic cells, was determined by flow cytometry (29) with some modifications. Briefly, the cells were treated with DATS as described above, fixed in 70% ethanol at 4°C, suspended in 1 mL of 0.25% Triton X-100 in PBS, and incubated on ice for 15 min. The cells were collected, suspended in 100 μL of PBS containing 1% BSA and 0.75 μg of a polyclonal anti–phospho-($Ser^{10}$)-histone H3 antibody, and incubated at 4°C overnight with gentle shaking. The cells were then rinsed with PBS containing 1% BSA and incubated in the dark with FITC-conjugated goat anti-rabbit antibody (1:50 dilution in PBS containing 1% BSA) for 45 min at room temperature. The cells were washed with PBS containing 1% BSA and treated with propidium iodide and RNase A for 30 min. Cellular fluorescence was measured using a Coulter Epics XL Flow Cytometer.

## Results

### DATS Treatment Delayed Mitotic Progression in Synchronized PC-3 Cells

We have shown previously that exposure of unsynchronized PC-3 cells to growth-suppressive concentrations of DATS (10, 20, and 40 μmol/L) results in a Chk1-dependent mitotic arrest characterized by the disruption of the α-tubulin network, chromatin condensation, and increased $Ser^{10}$ phosphorylation of histone H3 (24). The Chk1 is an intermediary of DNA damage checkpoint and is known to regulate DNA damage–induced S and $G_2$-M phase arrest (30–33). The Chk1 dependence of the DATS-mediated mitotic arrest observed in our model (24) resembled a newly described mitotic exit checkpoint in γ-irradiated HeLa cells (34), where nocodazole-synchronized HeLa cells exposed to γ-irradiation accumulated in the late telophase stage (34). We raised the question of whether DATS-mediated mitotic arrest in our model was due to the inhibition of mitotic exit. To address this question, we synchronized PC-3 cells in prometaphase stage by a 24-h treatment with 0.1 μg/mL nocodazole. The synchronized cells were released to fresh medium with or without 40 μmol/L DATS for 1, 2, or 4 h before analysis of cell morphology or cell cycle distribution. As can be seen in Fig. 1, nocodazole treatment resulted in the accumulation of cells with 4N DNA content ($G_2$-M population) mainly due to a reduction in $G_1$ and S phase cells. Fluorescence microscopic analysis of DAPI-stained cells confirmed that nocodazole-treated PC-3 cells were arrested in

Published OnlineFirst April 3, 2007; DOI: 10.1158/1535-7163.MCT-06-0477



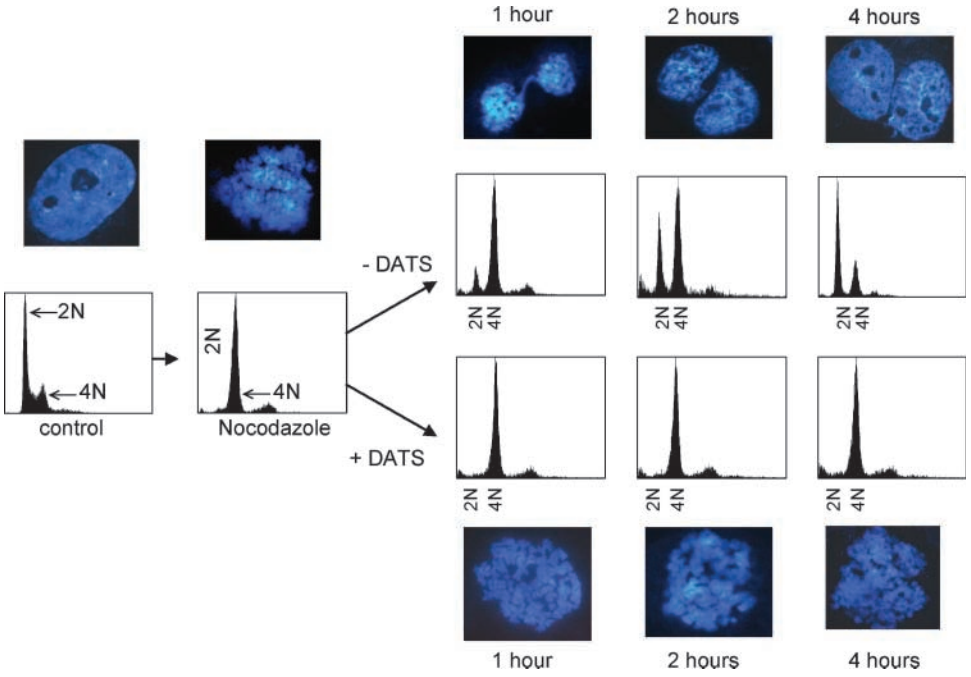


**Figure 1.** Representative histograms for cell cycle distribution in control or nocodazole-synchronized PC-3 cells (0.1 μg/mL for 24 h) and those released to normal medium or medium containing 40 μmol/L DATS for the indicated time periods. *Insets,* representative fluorescence microscopic images of DAPI-stained cells. Similar results were observed in two independent experiments.

prometaphase stage characterized by chromatin condensation and disruption of the nuclear envelope (Fig. 1). The cells released to normal medium after the removal of nocodazole restarted cycling as evidenced by the appearance of interphase cells (DAPI staining) and a progressive decrease in $G_2$-M fraction (4N DNA content) that was accompanied by an increase in $G_1$ phase cells (2N DNA content). However, synchronized PC-3 cells released to DATS-containing medium remained arrested in prometaphase stage (Fig. 1). For instance, 2 h after release to the control medium, ~24% cells exhibited $G_1$ phase DNA content, whereas the percentage of $G_1$ fraction in cells released to DATS-containing medium was only 2.5%. Even after 4 h of release, ~80% of the DATS-treated cells were unable to complete mitosis and contained 4N DNA content. By contrast, more than 58% of the control cells had completed mitosis after 4 h of release in medium lacking DATS. Unlike γ-irradiated HeLa cells which progressed to the telophase stage (34), the DATS-treated PC-3 cells were unable to progress beyond the prometaphase stage as judged by fluorescence microscopy after staining with DAPI (Fig. 1). These results indicated that the DATS-induced mitotic arrest observed in synchronized PC-3 cells (Fig. 1) was different from the mitotic exit checkpoint described previously for γ-irradiated HeLa cells (34).

### DATS Treatment Caused Accumulation of Substrates of APC/C and Phosphorylation of Cdc20 and Cdh1

Initiation of anaphase as well as mitotic exit depends on active APC/C, which is a multisubunit ubiquitin-protein ligase complex (35–38). To determine if DATS-mediated prometaphase arrest was due to the inactivation of APC/C, we compared the protein levels of known APC/C substrates (cyclin A, cyclin B1, and securin) by immunoblotting using lysates from PC-3 cells synchronized with nocodazole (0.1 μg/mL for 24 h) and released to medium containing DMSO (control) or 40 μmol/L DATS for 2 or 4 h. As expected, nocodazole-synchronized PC-3 cells expressed high levels of cyclin A, cyclin B1, and securin (Fig. 2A). The levels of cyclin A, cyclin B1, and securin proteins were reduced markedly in a time-dependent manner in cells released to control medium without DATS, which is an indication of active APC/C. However, cells released to DATS-containing medium maintained high levels of cyclin A, cyclin B1, and securin for the duration of the experiment (Fig. 2A). Interestingly, securin protein accumulation was accompanied by the appearance of a slower migrating band corresponding to the phosphorylated form of the protein. We also determined the levels of key APC/C subunits in nocodazole-synchronized cells as well as in cells released to control or DATS-containing medium by immunoblotting, and representative blots are shown in Fig. 2B. Cdc27 is one of the core subunits of APC/C, which becomes phosphorylated in mitosis (38). Nocodazole-synchronized PC-3 cells revealed characteristic mitotic phosphorylation pattern of Cdc27 protein (slower migrating band), which was reduced markedly in cells released to control medium. Hyperphosphorylation of Cdc27 was maintained in cells released to the DATS-containing medium, which confirmed that the DATS-treated cells were blocked in mitosis. The Cdc20 and Cdh1 are the regulatory subunits of APC/C responsible for substrate recognition by the holoenzyme (39, 40). Nocodazole-synchronized prometaphase cells contained phosphorylated Cdc20 (slower migrating bands), which was reduced in cells released to the control medium without DATS. Phosphorylation of Cdc20 was maintained in cells released

Published OnlineFirst April 3, 2007; DOI: 10.1158/1535-7163.MCT-06-0477



to the DATS-containing medium (Fig. 2B). Cdh1 is inactive when phosphorylated by Cdk1/cyclin B1 kinase complex, and its activation correlates with cyclin B1 degradation following dephosphorylation by Cdc14 phosphatase (41). The nocodazole-arrested cells revealed a slower migrating band of Cdh1 corresponding to its phosphorylated form, which disappeared in cells released to control medium. The phosphorylated form of Cdh1 was observed in cells released to the DATS-containing medium (Fig. 2B). Collectively, these results indicated that nocodazole-synchronized cells released to the DATS-containing medium were unable to complete mitosis possibly due to the inactivation of the APC/C.

### Dose Response and Time Course Kinetics of DATS-Induced Mitotic Arrest

We conducted a dose response study to further characterize DATS-induced mitotic arrest using unsynchronized PC-3 cells and by monitoring $Ser^{10}$ phosphorylation of histone H3 (a sensitive marker for mitotic cells) and hyperphosphorylation of APC/C substrate securin. As can be seen in Fig. 3A, the DATS-mediated hyperphosphorylation of both histone H3 and securin (fold changes in the levels of top band representing hyperphosphorylated securin are shown) was apparent following 8-h treatment of PC-3 cells with 10, 20, and 40 μmol/L concentrations. In a time course kinetic study, increased phosphorylation of histone H3 at $Ser^{10}$ in cells exposed to 40 μmol/L DATS was evident as early as 2 h after treatment compared with DMSO-treated control (Fig. 3B). Similarly, hyperphosphorylation of securin (quantitative data for the top band representing hyperphosphorylated form of securin are shown) was evident at the 4- to 8-h time points (Fig. 3B). These results indicated that DATS treatment caused mitotic arrest in unsynchronized PC-3 cells in a concentration- and time-dependent manner.

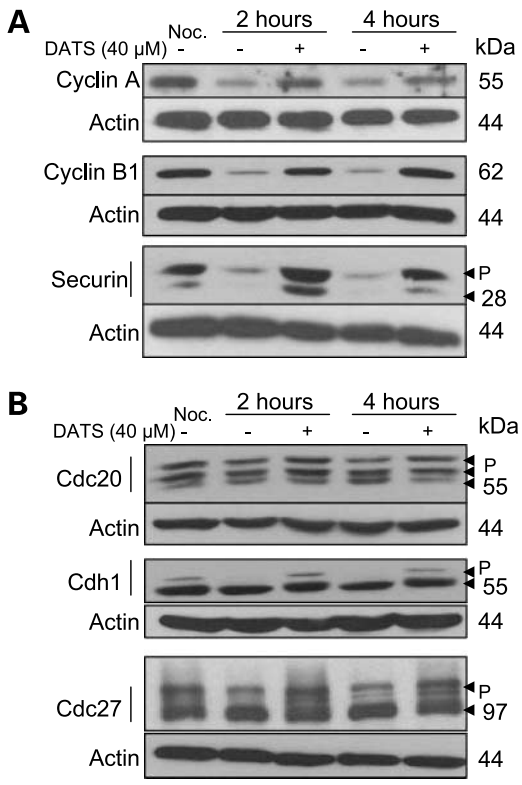


**Figure 2.** **A,** immunoblotting for APC/C substrates (cyclin A, cyclin B1, and securin) using lysates from control or nocodazole synchronized PC-3 cells (0.1 μg/mL for 24 h) and those released to normal medium or medium containing 40 μmol/L DATS for 2 or 4 h. **B,** immunoblotting for APC/C subunits (Cdc20, Cdh1, and Cdc27) using lysates from control or nocodazole synchronized PC-3 cells (0.1 μg/mL for 24 h) and those released to normal medium or medium containing 40 μmol/L DATS for 2 or 4 h. The blots were stripped and reprobed with anti-actin antibody to ensure equal protein loading. Similar results were observed in at least two experiments using independently prepared lysates. Note a progressive decrease in levels of cyclin A and cyclin B1 and as well as a decrease in the phosphorylation of APC/C subunits in nocodazole synchronized PC-3 cells released to normal medium, but not in cells released to DATS-containing medium. *P,* phosphorylated forms of different proteins.

To test if DATS-induced mitotic arrest was reversible, cells were first exposed to either DMSO (control) or 40 μmol/L DATS for 4 h at 37°C. Subsequently, the cells were either examined for mitotic fraction or washed and maintained in fresh complete medium without DMSO or DATS for an additional 2 or 4 h. The cells were then collected and processed for fluorescence microscopic analysis of prometaphase cells with chromatin condensation and disruption of the nuclear envelope (DAPI staining) or immunoblotting for phospho–($Ser^{10}$)-histone H3 and securin. As can be seen in Fig. 3C, a large fraction of DATS-treated cells was unable to complete mitosis even after 4 h of culture in drug-free medium as quantified by fluorescence microscopy after DAPI staining. The morphology of DAPI-stained nuclei of the released cells and the fact that DATS-mediated stabilization of cyclin B1, $Ser^{10}$ phosphorylation of histone H3, and hyperphosphorylation of securin were maintained for at least up to 4 h after drug removal (results not shown) point toward prometaphase arrest, because cell cycle progression beyond anaphase correlates with cyclin B1 degradation and dephosphorylation of histone H3. Collectively, these results indicated that a large fraction of DATS-treated cells were unable to progress beyond prometaphase at least for up to 4 h of culture in drug-free medium.

### Hyperphosphorylation of Cdc20 and Cdh1 Was Mediated by Chk1

We have shown previously that DATS-induced mitotic arrest in PC-3 and DU145 cells correlates with the activation of Chk1 (24), and the mitotic block caused by DATS is partially but significantly attenuated by knockdown of Chk1 protein using two independent siRNAs targeting distinct regions of Chk1 gene (24). To gain further insight into the mechanism by which Chk1 may contribute to DATS-mediated mitotic arrest, we determined the effect of Chk1 protein knockdown on protein levels/phosphorylation of APC/C substrates (cyclin B1 and securin) and its regulatory subunits (Cdc20 and Cdh1). Consistent with our previous data (24), DATS treatment (40 μmol/L for 8 h) caused a reduction in protein level of Chk1 in PC-3 cells transiently transfected with a control nonspecific siRNA. Moreover, Chk1 protein was barely detectable in PC-3 cells

Published OnlineFirst April 3, 2007; DOI: 10.1158/1535-7163.MCT-06-0477



transfected with Chk1-targeted siRNA confirming knockdown of Chk1 protein (Fig. 4). Similar to nocodazole-synchronized PC-3 cells (Fig. 2), DATS treatment caused a marked increase in the protein level of cyclin B1 and hyperphosphorylation of securin in control nonspecific siRNA-transfected PC-3 cells, which was reduced markedly in Chk1-depleted PC-3 cells. For instance, DATS treatment caused an approximate 5-fold increase in the levels of cyclin B1 protein in nonspecific control siRNA-transfected cells. A similar DATS treatment resulted in about a 2-fold increase in cyclin B1 protein level in cells transfected with Chk1-specific siRNA as judged by densitometric scanning of the immunoreactive bands and corrected for actin loading control (Fig. 4). Similarly, the DATS-mediated phosphorylation of securin was about 1.7-fold higher in control nonspecific siRNA-transfected cells compared with cells transfected with Chk1-specific siRNA (Fig. 4). These results indicated that DATS treatment might cause the inactivation of APC/C that is partially dependent on Chk1 kinase.

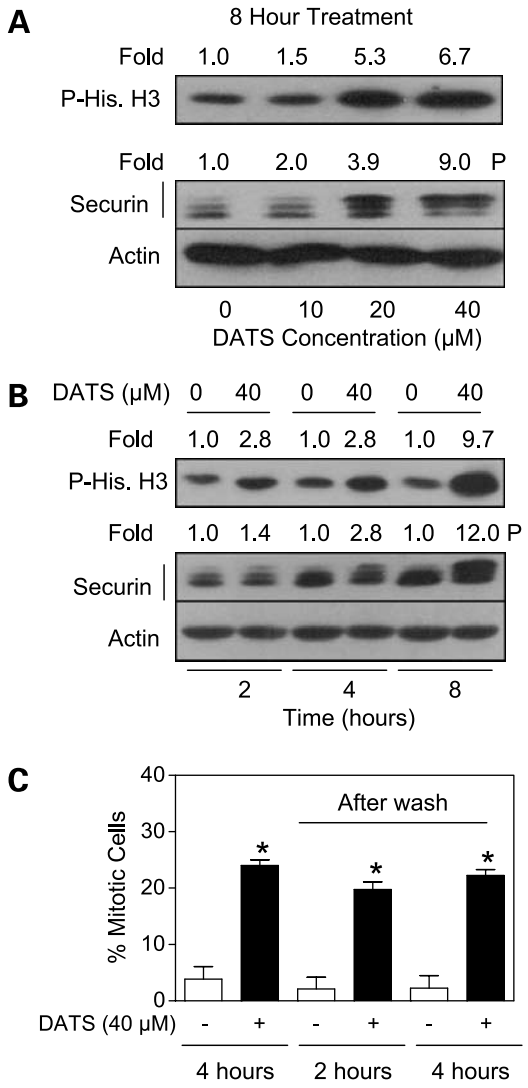


**Figure 3.** **A,** immunoblotting for the analysis of phospho – ($Ser^{10}$)-histone H3 and the phosphorylated form of securin using lysates from PC-3 cells treated for 8 h with DMSO (control) or the indicated concentrations of DATS. **B,** immunoblotting for phospho – ($Ser^{10}$)-histone H3 and the phosphorylated form of securin using lysates from PC-3 cells treated with DMSO (control) or 40 μmol/L DATS for the indicated time periods. The blots were stripped and reprobed with anti-actin antibody to ensure equal protein loading. *Numbers on top of the bands,* changes in protein levels determined by densitometric scanning of the immunoreactive bands and corrected for actin loading control. For securin, the quantitative data for the top band representing the hyperphosphorylated form of the protein (*P*) are shown in **A** and **B**. **C,** percentage of mitotic fraction in cells treated with DMSO (control) or 40 μmol/L DATS for 4 h and then maintained in drug-free fresh complete media for an additional 2 or 4 h after washing. The mitotic cells were scored by fluorescence microscopy after staining with DAPI. *Columns,* mean ($n = 3$); *bars,* SE. *, $P < 0.05$, significantly different compared with corresponding control by paired *t* test.

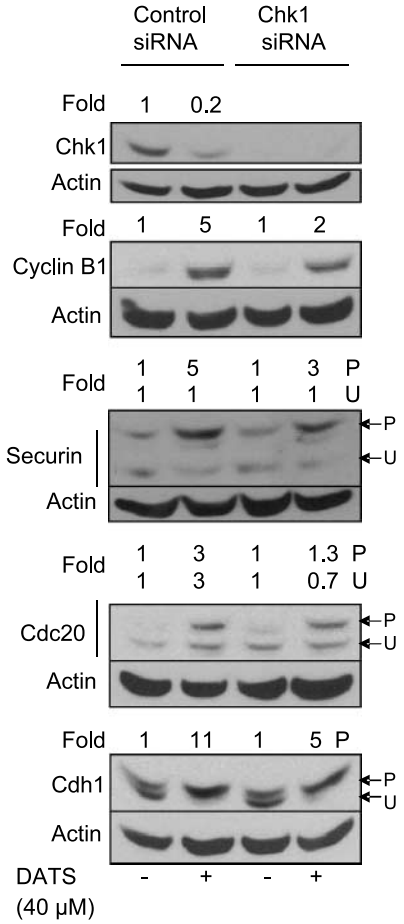


**Figure 4.** Immunoblotting for total Chk1, APC/C substrates (cyclin B1 and securin), and APC/C regulatory subunits (Cdc20 and Cdh1) using lysates from PC-3 cells transiently transfected with a nonspecific control siRNA or Chk1-specific siRNA and treated for 8 h with either DMSO (control) or 40 μmol/L DATS. The blots were stripped and reprobed with anti-actin antibody to ensure equal protein loading. Similar results were observed in replicate experiments. *P* and *U*, phosphorylated and unphosphorylated forms of different proteins, respectively. *Numbers on top of the immunoreactive bands,* changes in the levels of total and phosphorylated proteins, determined by densitometric scanning of the immunoreactive bands and corrected for actin loading control.

Published OnlineFirst April 3, 2007; DOI: 10.1158/1535-7163.MCT-06-0477



Next, we raised the question of whether the DATS-mediated hyperphosphorylation of APC/C subunits Cdc20 and Cdh1 was regulated by Chk1. To test this possibility, we determined the effect of Chk1 protein knockdown on DATS-mediated phosphorylation of Cdc20 and Cdh1. As can be seen in Fig. 4, DATS treatment caused an approximate 3- and 11-fold increase in the levels of phosphorylated Cdc20 and Cdh1, respectively, in control nonspecific siRNA-transfected PC-3 cells. The DATS-mediated phosphorylation of Cdc20 and Cdh1 was partially yet markedly reduced in Chk1 siRNA-transfected cells. These results suggested that DATS-induced phosphorylation of Cdc20 and Cdh1 might be mediated by Chk1 kinase.

### Expression of Kinase Dead ATR in U2OS Osteosarcoma Cells Partially Abrogated DATS-Induced Mitotic Arrest

To address the questions of (*a*) whether DATS-mediated and Chk1-dependent prometaphase arrest was restricted to the PC-3 cell line due to its unique characteristics and (*b*) whether DATS-induced activation of Chk1 was mediated by ATR, we determined the effect of DATS treatment on Chk1 activation ($Ser^{317}$ phosphorylation), accumulation of APC/C substrates (securin and cyclin B1), and phosphorylation of Cdc20 and Cdh1 using U2OS osteosarcoma cells expressing doxycycline-inducible and Flag-tagged wild-type (ATR-wt) or kinase dead ATR (ATR-kd). As can be seen in Fig. 5A, doxycycline treatment caused the induction of wild-type as well as kinase dead ATR proteins as judged by immunoblotting for Flag and ATR. The DATS-mediated $Ser^{317}$ phosphorylation (activation) of Chk1 was relatively more pronounced in ATR-wt cells than in kinase dead ATR-expressing cells. Moreover, DATS treatment caused the accumulation of cyclin B1 and hyperphosphorylation of securin in ATR-wt cells, but these effects were relatively less pronounced in ATR-kd cells (Fig. 5A). Similar to PC-3 cells (Fig. 4), DATS treatment caused an increase in phosphorylation of Cdc20 and Cdh1 in ATR-wt cells, which was relatively less pronounced in ATR-kd cells (Fig. 5B). Collectively, these results indicated that the DATS-induced accumulation/phosphorylation of APC/C substrates and phosphorylation of APC/C subunits Cdc20 and Cdh1 was not restricted to the PC-3 cell line, and that Chk1 phosphorylation (activation), upon treatment with DATS, was at least in part mediated by the ATR kinase.

Next, we determined the effect of DATS treatment (40 μmol/L for 4 or 8 h) on mitotic progression using ATR-wt and ATR-kd cells. Cells in different stages of mitosis in asynchronous cultures of DATS-treated ATR-wt and ATR-kd cells were examined by immunofluorescence microscopy following staining with α-tubulin and DAPI. Representative images of cells in different stages of mitosis (prometaphase, metaphase, anaphase, and telophase) in DMSO-treated (control) ATR-wt cultures are depicted in Fig. 6A. As can be seen in Fig. 6B, cells representing different stages of mitosis were observed in vehicle-treated control ATR-wt (*left*) as well as ATR-kd cells (*right*). In the presence of DATS, however, the ATR-wt cells were unable to progress beyond the prometaphase stage. On the other hand, the ATR-kd cells were able to proceed through different stages of mitosis even after treatment with DATS (Fig. 6B). Approximately 17% of DATS-treated ATR-wt cells exhibited multinucleation, which is a feature characteristic of mitotic catastrophe (Fig. 6C). Interestingly, the DATS-induced multinucleation was barely detectable in ATR-kd cells even after treatment with DATS (Fig. 6C). These results provided experimental evidence to indicate ATR/Chk1 dependence of DATS-induced prometaphase arrest.

We used ATR-targeted siRNA and DU145 cells to further characterize ATR/Chk1 dependence of mitotic arrest in our model. As can be seen in Fig. 7A, transient transfection of cells with an ATR-specific siRNA resulted in ~60%

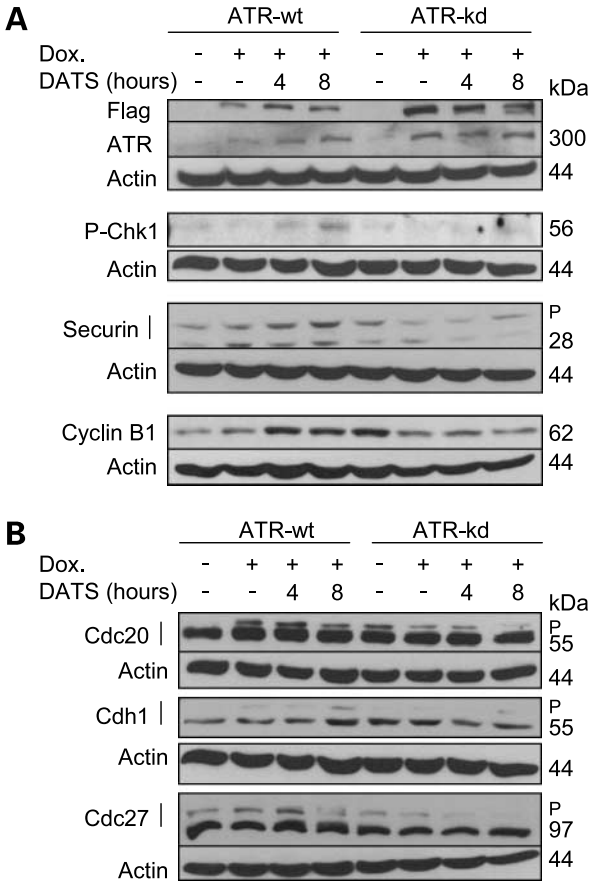


**Figure 5.** **A,** immunoblotting for Flag, ATR, phospho–($Ser^{317}$)-Chk1, and APC/C substrates (securin and cyclin B1) using lysates from U2OS osteosarcoma cells expressing doxycycline-inducible Flag-tagged wild-type ATR (ATR-wt) or kinase dead ATR (ATR-kd) following treatment with DMSO or DATS. The U2OS cells were treated with 1 μg/mL doxycycline for 48 h to induce expression of wild-type or kinase dead ATR. Subsequently, the cells were treated with DMSO or 40 μmol/L DATS for 4 or 8 h. **B,** immunoblotting for APC/C regulatory subunits (Cdc20, Cdh1, and Cdc27) using lysates from U2OS osteosarcoma cells expressing ATR-wt or ATR-kd following treatment with DMSO (control) or 40 μmol/L DATS for 4 or 8 h. The blots were stripped and reprobed with anti-actin antibody to ensure equal protein loading. *P,* phosphorylated forms of different proteins. Similar results were observed in at least two independent experiments.

Published OnlineFirst April 3, 2007; DOI: 10.1158/1535-7163.MCT-06-0477



knockdown of the ATR protein when compared with nonspecific control siRNA-transfected cells. The DATS-mediated activation ($Ser^{317}$ phosphorylation) of Chk1, accumulation of cyclin B1, phosphorylation of APC/C subunit Cdh1, and $Ser^{10}$ phosphorylation of histone H3 (mitotic marker) were much more pronounced in nonspecific control siRNA-transfected cells than in the cells transfected with the ATR-specific siRNA (Fig. 7B). For example, DATS treatment (40 μmol/L for 8 h) caused an approximate 7-fold increase in the levels of phospho–($Ser^{10}$)-histone H3 compared with DMSO-treated control in cells transiently transfected with a nonspecific control siRNA (Fig. 7B). On the other hand, a similar DATS treatment resulted in about 3-fold increase in $Ser^{10}$ phosphorylation of histone H3 in cells with ATR knockdown (Fig. 7B). Collectively, these results indicated that the DATS-mediated prometaphase arrest was, at least in part, dependent on ATR/Chk1 pathway.

### Securin Was Dispensable for DATS-Induced Mitotic Arrest

Securin is known to regulate mitotic progression by functioning as inhibitor of sister-chromatid separation (42–45). Because DATS treatment resulted in the accumulation as well as emergence of slower migrating bands of securin (Figs. 2 and 3), we designed experiments to determine the possible role of this protein in DATS-mediated prometaphase arrest. Initially, we tested the possibility whether the slower migrating bands of securin represented phosphorylated forms of the protein. As can be seen in Fig. 8A, the DATS-mediated accumulation of slower migrating bands of securin was abolished if the lysate was treated with λ protein phosphatase before immunoblotting, confirming the phosphorylation of securin. Next, we used siRNA technology to determine the role of securin in DATS-induced prometaphase arrest. DATS treatment caused the accumulation of phosphorylated securin in control siRNA-transfected PC-3 cells. The securin protein was barely detectable in PC-3 cells transfected with securin-specific siRNA even after treatment with DATS (Fig. 8B), thus confirming knockdown of securin protein. Interestingly, the securin protein knockdown did not have any appreciable effect on DATS-mediated accumulation of cyclin B1 (Fig. 8B). These results suggested that the depletion of securin protein might not be able to rescue cells from DATS-induced mitotic arrest. We verified this speculation by determining the effect of DATS treatment on $Ser^{10}$ phosphorylation of histone H3 by flow cytometry in PC-3 cells transfected with a control nonspecific siRNA and securin-specific siRNA 1. As can be seen in Fig. 8C, the DATS-mediated increase in $Ser^{10}$ phosphorylation of

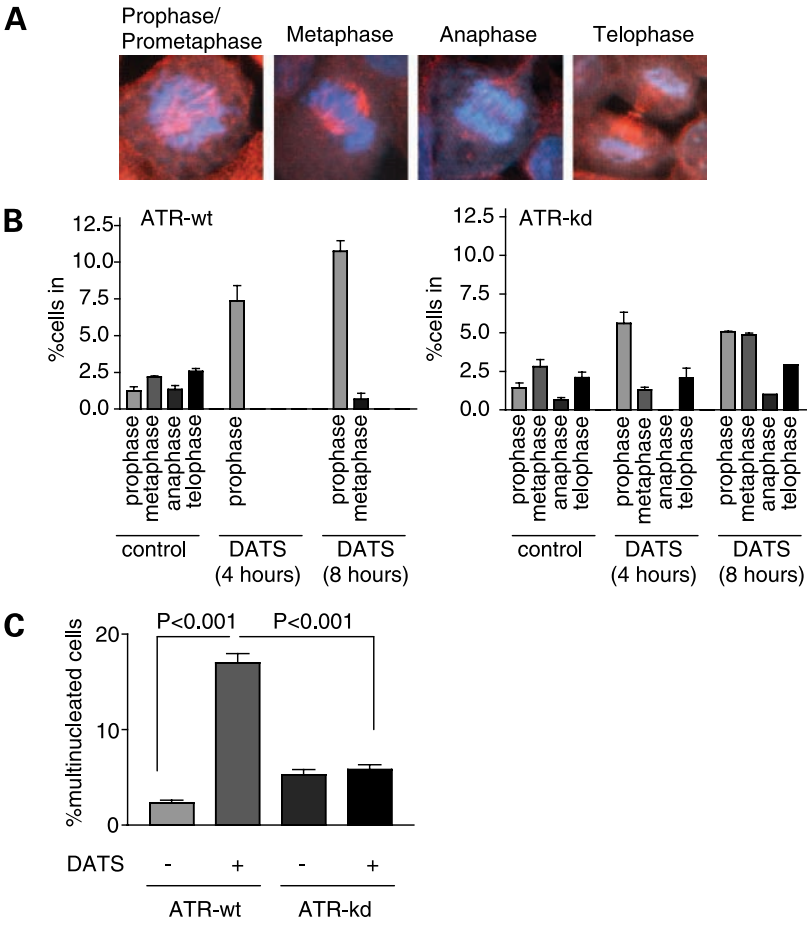


**Figure 6.** **A,** representative fluorescence microscopic images of U2OS osteosarcoma cells expressing doxycycline-inducible wild-type ATR depicting different stages of mitosis (prometaphase, metaphase, anaphase, and telophase) judged by α-tubulin (*red fluorescence*) and DAPI (*blue fluorescence*) staining. **B,** percentage of cells in different stages of mitosis in U2OS osteosarcoma cells expressing doxycycline-inducible and Flag-tagged wild-type ATR (ATR-wt) or kinase dead ATR (ATR-kd) following treatment with 40 μmol/L DATS for 4 or 8 h. The U2OS cells were treated with 1 μg/mL doxycycline for 48 h to induce expression of wild-type or kinase dead ATR. Subsequently, the cells were treated with DMSO (control) or 40 μmol/L DATS for 4 or 8 h. Cells in different stages of mitosis were scored under a fluorescence microscope following staining with anti–α-tubulin antibody and DAPI. A total of 500 cells from different slides were scored for mitotic cells. Experiment was repeated twice with similar results. **C,** percentage of multinucleated cells in U2OS osteosarcoma cells expressing ATR-wt or ATR-kd following treatment with DMSO or 40 μmol/L DATS for 24 h. Multinucleated cells were scored under a fluorescence microscope following staining with anti–α-tubulin antibody and DAPI. A total of 600 to 700 cells from slides were scored for multinucleated cells. Experiment was repeated twice with similar results. For data in **B** and **C**, *columns,* mean ($n$ = 3); *bars*, SE. Statistical significance of the difference in DATS-mediated accumulation of multinucleated cells between ATR-wt and ATR-kd (**C**) was assessed by one-way ANOVA followed by Bonferroni's multiple comparison test.

Published OnlineFirst April 3, 2007; DOI: 10.1158/1535-7163.MCT-06-0477



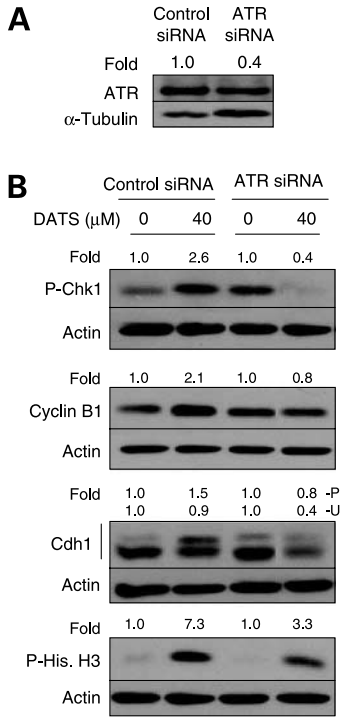


**Figure 7.** **A,** immunoblotting for ATR protein in DU145 cells transiently transfected with a nonspecific control siRNA or ATR-targeted siRNA. **B,** immunoblotting for phospho – (Ser$^{317}$)-Chk1, APC/C substrate cyclin B1, APC/C regulatory subunit Cdh1, and mitotic marker phospho – (Ser$^{10}$)-histone H3 using lysates from DU145 cells transiently transfected with a nonspecific control siRNA or ATR-specific siRNA and treated for 8 h with either DMSO (control) or 40 μmol/L DATS. The blots were stripped and reprobed with anti – α-tubulin antibody or anti-actin antibody to ensure equal protein loading. Similar results were observed in replicate experiments. *P* and *U*, phosphorylated and unphosphorylated forms of Cdh1, respectively. *Numbers on top of the immunoreactive bands,* changes in the levels of total and phosphorylated proteins, determined by densitometric scanning of the immunoreactive bands and corrected for actin loading control.

histone H3 was observed in PC-3 cells transfected with control nonspecific siRNA and securin-targeted siRNA 1. We used a second securin-specific siRNA 2 to rule out the possibility of an off-target effect. Similar to experiments using securin siRNA 1, the DATS-mediated mitotic arrest was maintained in cells with more than 90% depletion of securin protein (Fig. 8D) using siRNA 2 as judged by flow-cytometric analysis of Ser$^{10}$ phosphorylated histone H3 (Fig. 8E). These results suggested that securin protein stabilization and phosphorylation were a consequence rather than a cause of DATS-induced mitotic arrest.

## Discussion

The present study describes an ATR/Chk1-dependent signaling pathway partially responsible for DATS-induced prometaphase arrest in cancer cells (Fig. 9). The DATS-mediated and ATR/Chk1-dependent prometaphase arrest seems to be caused by the inactivation of APC/C. The activity of APC/C is regulated by reversible phosphorylation of its components as well as interaction between APC/C core and the regulatory subunits Cdc20 and Cdh1, which are responsible for substrate recognition by the holoenzyme (39). For instance, the APC/Cdc20 ubiquitinates cyclin A, securin, and part of the cyclin B1 pool, which drives cells to anaphase (39). During mitotic exit, Cdc20 is replaced by Cdh1, and the APC/Cdh1 complex ubiquitinates rest of the cyclin B1 pool, Cdc20 itself, and other mitotic kinases, including Aurora kinase and polo-like kinase 1 (39, 40). The present study reveals that the DATS-mediated inactivation of APC/C is partially linked to Chk1 activation, but not restricted to the PC-3 cell line. This conclusion is supported by the following observations: (*a*) DATS treatment causes the accumulation of APC/C substrates, including cyclin A, cyclin B1, and securin in PC-3 (Fig. 2A) and U2OS cells (Fig. 5A); (*b*) the DATS-mediated accumulation of APC/C substrates in PC-3 cells is partially but markedly suppressed by knockdown of Chk1 protein (Fig. 4), and we have shown previously that Chk1 protein depletion confers partial yet statistically significant protection against DATS-mediated mitotic arrest (24); (*c*) unlike ATR-wt cells, the ATR-kd cells are able to proceed through telophase even after treatment with DATS (Fig. 6B); and (*d*) ATR knockdown offers partial protection against DATS-induced mitotic arrest (Fig. 7). However, the possibility that the DATS-induced prometaphase arrest is also regulated by ATR/Chk1-independent mechanism(s) cannot be ignored because >90% depletion of the Chk1 protein confers only partial protection against the DATS-mediated accumulation of APC/C substrates (present study) as well as mitotic arrest (24).

Using HeLa cells as a model, Huang et al. (34) have very recently provided experimental evidence to indicate involvement of Chk1 in the regulation of DNA damage-induced (γ-irradiation) mitotic exit (34). The Chk1-dependent mitotic exit checkpoint observed in HeLa cells, however, is strikingly different from the prometaphase checkpoint observed in our model. First, the DATS-treated cells fail to proceed beyond the prometaphase stage, whereas the HeLa cells are able to enter anaphase, but unable to exit mitosis as revealed by the accumulation of the late telophase cells (34). The metaphase-anaphase transition of HeLa cells is also supported by a lack of stabilization of APC/C substrate securin (34), which is stabilized as well as phosphorylated in DATS-treated cells (present study).

Immunoblotting for APC/C subunits Cdc20 and Cdh1 suggested their phosphorylation (slower migrating bands) in DATS-treated PC-3 cells (Fig. 4) and wild-type ATR-expressing U2OS osteosarcoma cells (Fig. 5B). Phosphorylation of Cdc20 has been shown to inhibit the activity of APC/C during spindle checkpoint induction (46–48). In addition, Cdh1 phosphorylation inhibits its binding to APC/C core, and Cdh1 is dephosphorylated before mitotic exit (41). It is interesting to note that the interference of Chk1 activation, either by siRNA-based knockdown of Chk1/ATR proteins (Figs. 4 and 7) or by overexpression of kinase dead ATR (Fig. 5B), partially protects against DATS-induced phosphorylation of Cdc20 and Cdh1. These results suggest that Chk1 may, either directly or indirectly, cause

Published OnlineFirst April 3, 2007; DOI: 10.1158/1535-7163.MCT-06-0477



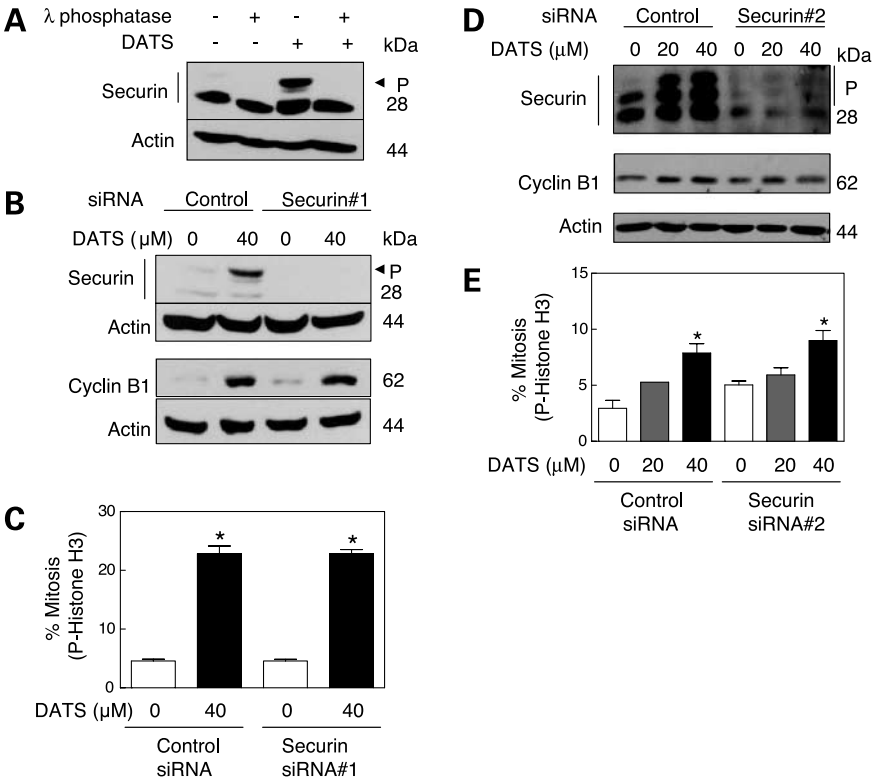


**Figure 8.** **A,** immunoblotting for securin protein using lysates from control (DMSO-treated, 8 h) and DATS-treated (40 μmol/L DATS for 8 h) PC-3 cells with or without a 4-h pretreatment with λ protein phosphatase. **B,** immunoblotting for securin and cyclin B1 using lysates from PC-3 cells transiently transfected with a nonspecific control siRNA or a securin-specific siRNA (siRNA 1) and treated for 8 h with either DMSO (control) or 40 μmol/L DATS. **C,** percentage of mitotic cells, judged by flow-cytometric analysis of $Ser^{10}$ phosphorylated histone H3 (a mitotic marker), in PC-3 cultures transiently transfected with a nonspecific control siRNA or a securin-specific siRNA (siRNA 1) and treated for 8 h with either DMSO (control) or 40 μmol/L DATS. **D,** immunoblotting for securin and cyclin B1 using lysates from PC-3 cells transiently transfected with a nonspecific control siRNA or pool of three securin-specific 20- to 25-nt siRNA (siRNA 2) and treated for 8 h with either DMSO (control) or DATS (20 or 40 μmol/L). **E,** percentage of mitotic cells, judged by flow-cytometric analysis of $Ser^{10}$ phosphorylated histone H3 (a mitotic marker), in PC-3 cultures transiently transfected with a nonspecific control siRNA or a pool of three securin-specific, 20- to 25-nt siRNA (siRNA 2) and treated for 8 h with either DMSO (control) or DATS (20 or 40 μmol/L). In **C** and **E**, *columns*, mean ($n = 3-4$); *bars*, SE. *, $P < 0.05$, significantly different compared with corresponding DMSO-treated control by paired *t* test. In **A, B**, and **D**, the blots were stripped and reprobed with anti-actin antibody to ensure equal protein loading. Similar results were observed in replicate experiments.

phosphorylation of Cdc20 and Cdh1, leading to the inhibition of APC/C. However, further studies are needed to determine whether Cdc20 and/or Cdh1 are direct substrates of Chk1, or the Chk1-mediated phosphorylation of Cdc20 and Cdh1 is mediated by other intermediary kinases. For example, the phosphorylation of Cdc20 by Bub1 provides a catalytic mechanism for APC/C inhibition by the spindle checkpoint (48). The checkpoint protein BubR1 acts synergistically with Mad2 to inhibit APC/C (49). We considered the possibility whether Chk1-dependent phosphorylation of Cdc20 is mediated by BubR1. We found that DATS treatment causes phosphorylation of BubR1 in PC-3 cells, which is maintained in cells transfected with a Chk1-specific siRNA.[1] These results suggest that DATS-induced and Chk1-dependent phosphorylation of Cdc20 in our model may not be mediated by BubR1.

The Chk1 kinase is an intermediary of DNA damage checkpoint and activated by ATR in response to different stimuli (reviewed in ref. 50). A fundamental question, which remains unanswered, is how DATS treatment activates ATR/Chk1 signaling pathway. Based on available experimental evidence, we are tempted to postulate that the activation of ATR/Chk1 in DATS-treated prostate cancer cells is probably linked to the generation of ROS. This speculation is based on the following observations: (*a*) the DATS-induced cell cycle arrest in PC-3 and DU145 cells correlates with ROS generation due to an increase in the labile iron pool (22, 26); (*b*) pretreatment of cells with desferrioxamine, an iron chelator, confers significant protection against both DATS-mediated ROS generation and cell cycle arrest (26); (*c*) DATS treatment causes an increase in phosphorylation of histone H2A.X at $Ser^{139}$ (24), a sensitive marker for DNA double-strand breaks; and (*d*) ROS can directly cause DNA damage as well as oxidize nucleotides that can be converted to double-strand breaks during DNA replication (51, 52). However, further studies

[1] A. Herman-Antosiewicz, and S.V. Singh, unpublished observations.

Published OnlineFirst April 3, 2007; DOI: 10.1158/1535-7163.MCT-06-0477



are needed to firmly establish if the activation of ATR/Chk1 in our model is linked to ROS generation or caused by other mechanisms possibly involving direct interaction with DATS or ROS-dependent redox modification of other auxiliary proteins.

Chk1 involvement in the regulation of mitotic transition has been reported in *Saccharomyces cerevisiae* (53–56) and *Drosophila melanogaster* (57). It has been shown that Chk1 can directly phosphorylate securin, which leads to its stabilization and pre-anaphase arrest. In addition to the inhibition of sister chromatid separation, securin negatively controls the degradation of mitotic cyclins by inhibiting Cdh1 dephosphorylation (58). In the present study, we considered the possibility whether Chk1-mediated phosphorylation of securin contributes to DATS-mediated prometaphase arrest. The DATS-mediated phosphorylation of securin is significantly attenuated by RNA interference of Chk1 in PC-3 cells (Fig. 4) as well as the overexpression of kinase dead ATR in U2OS cells (Fig. 5A). These results indicate that phosphorylation of securin in DATS-treated cells is indeed caused by ATR/Chk1. We also found that securin protein physically interacts with Chk1 as revealed by immunoprecipitation of the securin protein followed by immunoblotting for Chk1 (results not shown). Moreover, the interaction between Chk1 and securin is exacerbated in DATS-treated PC-3 cells (results not shown). However, in our model, the phosphorylation of securin is an effect of ATR/Chk1 activation rather than the cause of DATS-induced prometaphase arrest because knockdown of securin protein using two different siRNA fails to protect against DATS-induced mitotic arrest (Fig. 8).

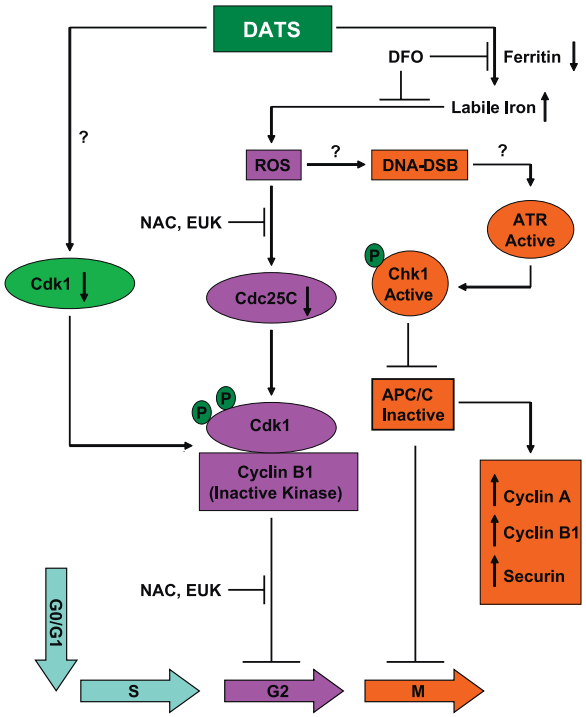


**Figure 9.** Proposed mechanisms explaining DATS-induced $G_2$ and M phase cell cycle arrest in human prostate cancer cells based on the results of the present study and our previous observations (22, 24, 26). We have shown previously that DATS treatment causes degradation of ferritin leading to the elevation of labile (chelatable) iron pool and ROS generation in PC-3 and DU145 cells (26). The DATS-mediated ROS generation is inhibited in the presence of the iron chelator desferrioxamine (*DFO*; ref. 26). The DATS-induced $G_2$ phase cell cycle arrest correlates with the ROS-dependent destruction of Cdc25C, which is reversible in the presence of antioxidants *N*-acetylcysteine (*NAC*) and combined catalase and superoxide dismutase mimetic EUK134 (*EUK*), and down-regulation of Cdk1 protein (22). The mechanism for DATS-mediated down-regulation of Cdk1 protein expression is not yet clear, but the net result of these effects is the accumulation of inactive ($Tyr^{15}$ phosphorylated Cdk1) Cdk1/cyclin B1 kinase complex (24). The present study reveals the existence of an ATR/Chk1-dependent mechanism partially responsible for DATS-mediated prometaphase arrest in cancer cells, which correlates with the inactivation of APC/C as evidenced by the accumulation of its substrates cyclin A, cyclin B1, and securin. The mechanism by which DATS may cause the activation of ATR remains elusive, but may involve ROS-dependent DNA double-strand breaks (*DNA-DSB*).

The DATS-mediated cell growth inhibition and cell cycle arrest is observed at concentrations (10, 20, and 40 μmol/L) within the range pharmacologically achievable based on a recent pharmacokinetic study (59). The peak plasma concentration of DATS in rats following treatment with 10 mg DATS has been shown to be about 31 μmol/L (59). Although the pharmacokinetic parameters for DATS in humans have not yet been measured, p.o. administration of 200 mg of synthetic DATS (referred to as allitridum), in combination with 100 μg selenium every other day for 1 month to humans, did not cause any harmful side effects (60). It is therefore possible that the plasma concentrations of DATS required for cancer cell growth inhibition may be achievable in humans.

Processing (cutting or chewing) of garlic and other *Allium* vegetables generates a number of OSCs besides DATS, including DAS, DADS, dipropyl sulfide, dipropyl disulfide, *S*-allylcysteine, *S*-allylmercaptocysteine, and ajoene (5). Although the effects of *S*-allylcysteine, *S*-allylmercaptocysteine, and ajoene on cell growth or cell cycle progression in prostate cancer cells have not been determined, we have shown previously that DATS is a much more potent suppressor of prostate cancer cell growth and/or cell cycle progression compared with DAS, DADS, dipropyl sulfide, and dipropyl disulfide, indicating that even a subtle change in organosulfide structure (e.g., the oligosulfide chain length in DAS and DADS versus DATS) could have a significant impact on its antiproliferative activity (21, 22). Without direct comparison of cellular effects (e.g., inhibition of cell growth and cell cycle progression) of different sulfur compounds generated by processing of garlic or other *Allium* vegetables in prostate cancer cells, it is difficult to gauge the relative contribution of DATS to the prostate cancer–protective effects of these vegetables. However, we can conclude with reasonable comfort that DATS probably plays a major role in anticancer effects of *Allium* vegetables, at least against prostate cancer, due to its relatively higher potency compared with DAS, DADS, dipropyl sulfide, and dipropyl disulfide (21, 22).

To summarize, data presented in this paper indicate that (*a*) DATS activates a prometaphase checkpoint in cancer

cells, which is not a cell line–specific effect; (*b*) the prometaphase checkpoint activation by DATS is partially dependent on the activation of ATR-Chk1 pathway; and (*c*) although securin is phosphorylated and stabilized in an ATR-Chk1–dependent manner, it reflects a downstream effect of activated Chk1 and is not responsible for DATS-mediated mitotic block.

**Acknowledgments**

The authors are grateful to Dr. P. Nghiem for the generous gift of U2OS osteosarcoma cells with doxycycline-inducible expression of wild-type ATR and kinase dead ATR. Technical assistance of Shoghag Panjarian is greatly appreciated.

**References**

**1.** You WC, Blot WJ, Chang YS, et al. *Allium* vegetables and reduced risk of stomach cancer. J Natl Cancer Inst 1989;18:162 – 4.

**2.** Gao CM, Takezaki T, Ding JH, Li MS, Tajima K. Protective effect of *Allium* vegetables against both esophageal and stomach cancer: a simultaneous case-referent study of a high-epidemic area in Jiangsu Province, China. Jpn J Cancer Res 1999;90:614 – 21.

**3.** Fleischauer AT, Poole C, Arab L. Garlic consumption and cancer prevention: meta-analyses of colorectal and stomach cancers. Am J Clin Nutr 2000;72:1047 – 52.

**4.** Hsing AW, Chokkalingam AP, Gao YT, et al. *Allium* vegetables and risk of prostate cancer: a population-based study. J Natl Cancer Inst 2002;94: 1648 – 51.

**5.** Block E. The organosulfur chemistry of the genus *Allium* — implications for the organic chemistry of sulfur. Angew Chem Int Ed Engl 1992;31: 1135 – 78.

**6.** Wargovich MJ. Diallyl sulfide, a flavor component of garlic (*Allium sativum*), inhibits dimethylhydrazine-induced colon cancer. Carcinogenesis 1987;8:487 – 9.

**7.** Sparnins VL, Barany G, Wattenberg LW. Effects of organosulfur compounds from garlic and onions on benzo(*a*)pyrene-induced neoplasia and glutathione *S*-transferase activity in the mouse. Carcinogenesis 1988; 9:131 – 4.

**8.** Wargovich MJ, Woods C, Eng VWS, Stephens LC, Gray K. Chemoprevention of *N*-nitrosomethylbenzylamine-induced esophageal cancer in rats by the naturally occurring thioether, diallyl sulfide. Cancer Res 1988; 48:6872 – 5.

**9.** Reddy BS, Rao CV, Rivenson A, Kelloff G. Chemoprevention of colon carcinogenesis by organosulfur compounds. Cancer Res 1993;53: 3493 – 8.

**10.** Schaffer EM, Liu JZ, Green J, Dangler CA, Milner JA. Garlic and associated allyl sulfur components inhibit *N*-methyl-*N*-nitrosourea induced rat mammary carcinogenesis. Cancer Lett 1996;102:199 – 204.

**11.** Hu X, Benson PJ, Srivastava SK, et al. Glutathione *S*-transferases of female A/J mouse liver and forestomach and their differential induction by anti-carcinogenic organosulfides from garlic. Arch Biochem Biophys 1996; 336:199 – 214.

**12.** Singh SV, Pan SS, Srivastava SK, et al. Differential induction of NAD(P)H:quinone oxidoreductase by anti-carcinogenic organosulfides from garlic. Biochem Biophys Res Commun 1998;244:917 – 20.

**13.** Brady JF, Ishizaki H, Fukuto JM, et al. Inhibition of cytochrome P-450 2E1 by diallyl sulfide and its metabolites. Chem Res Toxicol 1991; 4:642 – 7.

**14.** Singh SV. Impact of garlic organosulfides on p21(H-ras) processing. J Nutr 2001;131:1046 – 8s.

**15.** Xiao D, Lew KL, Kim Y, et al. Diallyl trisulfide suppresses growth of PC-3 human prostate cancer xenograft *in vivo* in association with Bax and Bak induction. Clin Cancer Res 2006;15:6836 – 43.

**16.** Sundaram SG, Milner JA. Diallyl disulfide induces apoptosis of human colon tumor cells. Carcinogenesis 1996;17:669 – 73.

**17.** Nakagawa H, Tsuta K, Kiuchi K, et al. Growth inhibitory effects of diallyl disulfide on human breast cancer cell lines. Carcinogenesis 2001; 22:891 – 7.

**18.** Xiao D, Pinto JT, Soh JW, et al. Induction of apoptosis by the garlic-derived compound *S*-allylmercaptocysteine (SAMC) is associated with microtubule depolymerization and c-Jun $NH_2$-terminal kinase 1 activation. Cancer Res 2003;63:6825 – 37.

**19.** Filomeni G, Aquilano K, Rotilio G, Ciriolo MR. Reactive oxygen species-dependent c-Jun $NH_2$-terminal kinase/c-Jun signaling cascade mediates neuroblastoma cell death induced by diallyl disulfide. Cancer Res 2003;63:5940 – 9.

**20.** Herman-Antosiewicz A, Singh SV. Signal transduction pathways leading to cell cycle arrest and apoptosis induction in cancer cells by *Allium* vegetable – derived organosulfur compounds: a review. Mutat Res 2004;555:121 – 31.

**21.** Xiao D, Choi S, Johnson DE, et al. Diallyl trisulfide-induced apoptosis in human prostate cancer cells involves c-Jun N-terminal kinase and extracellular-signal regulated kinase-mediated phosphorylation of Bcl-2. Oncogene 2004;23:5594 – 606.

**22.** Xiao D, Herman-Antosiewicz A, Antosiewicz J, et al. Diallyl trisulfide-induced $G_2$-M phase cell cycle arrest in human prostate cancer cells is caused by reactive oxygen species – dependent destruction and hyperphosphorylation of Cdc25C. Oncogene 2005;24:6256 – 68.

**23.** Hosono T, Fukao T, Ogihara J, et al. Diallyl trisulfide suppresses the proliferation and induces apoptosis of human colon cancer cells through oxidative modification of β-tubulin. J Biol Chem 2005;280: 41487 – 93.

**24.** Herman-Antosiewicz A, Singh SV. Checkpoint kinase 1 regulates diallyl trisulfide-induced mitotic arrest in human prostate cancer cells. J Biol Chem 2005;280:28519 – 28.

**25.** Xiao D, Singh SV. Diallyl trisulfide, a constituent of processed garlic, inactivates Akt to trigger mitochondrial translocation of BAD and caspase-mediated apoptosis in human prostate cancer cells. Carcinogenesis 2006; 27:533 – 40.

**26.** Antosiewicz J, Herman-Antosiewicz A, Marynowski SW, Singh SV. c-Jun $NH_2$-terminal kinase signaling axis regulates diallyl trisulfide-induced generation of reactive oxygen species and cell cycle arrest in human prostate cancer cells. Cancer Res 2006;66:5379 – 86.

**27.** Xiao D, Li M, Herman-Antosiewicz A, et al. Diallyl trisulfide inhibits angiogenic features of human umbilical vein endothelial cells by causing Akt inactivation and down-regulation of VEGF and VEGF-R2. Nutr Cancer 2006;55:94 – 107.

**28.** Nghiem P, Park PK, Kim Y, Vaziri C, Schreiber SL. ATR inhibition selectively sensitizes $G_1$ checkpoint-deficient cells to lethal premature chromatin condensation. Proc Natl Acad Sci U S A 2001;98:9092 – 7.

**29.** Widrow RJ, Laird CD. Enrichment for submitotic cell populations using flow cytometry. Cytometry 2000;39:126 – 30.

**30.** Sanchez Y, Wong C, Thoma RS, et al. Conservation of the Chk1 checkpoint pathway in mammals: linkage of DNA damage to Cdk regulation through Cdc25. Science 1997;277:1497 – 501.

**31.** Liu Q, Guntuku S, Cui XS, et al. Chk1 is an essential kinase that is regulated by Atr and required for the G(2)/M DNA damage checkpoint. Genes Dev 2000;14:1448 – 59.

**32.** Zhao H, Piwnica-Worms H. ATR-mediated checkpoint pathways regulate phosphorylation and activation of human Chk1. Mol Cell Biol 2001;21:4129 – 39.

**33.** Zhao H, Watkins JL, Piwnica-Worms H. Disruption of the checkpoint kinase 1/cell division cycle 25A pathway abrogates ionizing radiation-induced S and $G_2$ checkpoints. Proc Natl Acad Sci U S A 2002;99: 14795 – 800.

**34.** Huang X, Tran T, Zhang L, Hatcher R, Zhang P. DNA damage-induced mitotic catastrophe is mediated by the Chk1-dependent mitotic exit DNA damage checkpoint. Proc Natl Acad Sci U S A 2005;102: 1065 – 70.

**35.** Sudakin V, Ganoth D, Dahan A, et al. The cyclosome, a large complex containing cyclin-selective ubiquitin ligase activity, targets cyclins for destruction at the end of mitosis. Mol Biol Cell 1995;6:185 – 97.

**36.** King RW, Peters JM, Tugendreich S, Rolfe M, Hieter P, Kirschner MW. A 20S complex containing CDC27 and CDC16 catalyzes the mitosis-specific conjugation of ubiquitin to cyclin B. Cell 1995;81:279 – 88.

**37.** Zachariae W, Shin TH, Galova M, Obermaier B, Nasmyth K. Identification of subunits of the anaphase-promoting complex of *Saccharomyces cerevisiae*. Science 1996;274:1201 – 4.

**38.** Kraft C, Herzog F, Gieffers C, et al. Mitotic regulation of the human anaphase-promoting complex by phosphorylation. EMBO J 2003;22: 6598 – 609.

Published OnlineFirst April 3, 2007; DOI: 10.1158/1535-7163.MCT-06-0477



**39.** Peters JM. The anaphase-promoting complex: proteolysis in mitosis and beyond. Mol Cell 2002;9:931 – 43.

**40.** Lindon C, Pines J. Ordered proteolysis in anaphase inactivates Plk1 to contribute to proper mitotic exit in human cells. J Cell Biol 2004;164: 233 – 41.

**41.** Bembenek J, Yu H. Regulation of the anaphase-promoting complex by the dual specificity phosphatase human Cdc14a. J Biol Chem 2001;276: 48237 – 42.

**42.** Cohen-Fix O, Peters JM, Kirschner MW, Koshland D. Anaphase initiation in *Saccharomyces cerevisiae* is controlled by the APC-dependent degradation of the anaphase inhibitor Pds1p. Genes Dev 1996;10:3081 – 93.

**43.** Yamamoto A, Guacci V, Koshland D. Pds1p, an inhibitor of anaphase in budding yeast, plays a critical role in the APC and checkpoint pathway(s). J Cell Biol 1996;133:99 – 110.

**44.** Funabiki H, Yamano H, Kumada K, Nagao K, Hunt T, Yanagida M. Cut2 proteolysis required for sister-chromatid separation in fission yeast. Nature 1996;381:438 – 41.

**45.** Zou H, McGarry TJ, Bernal T, Kirschner MW. Identification of a vertebrate sister-chromatid separation inhibitor involved in transformation and tumorigenesis. Science 1999;285:418 – 22.

**46.** Yudkovsky Y, Shteinberg M, Listovsky T, Brandeis M, Hershko A. Phosphorylation of Cdc20/fizzy negatively regulates the mammalian cyclosome/APC in the mitotic checkpoint. Biochem Biophys Res Commun 2000;271:299 – 304.

**47.** D'Angiolella V, Mari C, Nocera D, Rametti L, Grieco D. The spindle checkpoint requires cyclin-dependent kinase activity. Genes Dev 2003;17: 2520 – 5.

**48.** Tang Z, Shu H, Oncel D, Chen S, Yu H. Phosphorylation of Cdc20 by Bub1 provides a catalytic mechanism for APC/C inhibition by the spindle checkpoint. Mol Cell 2004;16:387 – 97.

**49.** Fang G. Checkpoint protein BubR1 acts synergistically with Mad2 to inhibit anaphase-promoting complex. Mol Biol Cell 2002;13:755 – 66.

**50.** Yang J, Yu Y, Hamrick HE, Duerksen-Hughes PJ. ATM, ATR and DNA-PK: initiators of the cellular genotoxic stress responses. Carcinogenesis 2003;24:1571 – 80.

**51.** Galli A, Schiestl RH. Effects of DNA double-strand and single-strand breaks on intrachromosomal recombination events in cell-cycle – arrested yeast cells. Genetics 1998;149:1235 – 50.

**52.** Haber JE. DNA recombination: the replication connection. Trends Biochem Sci 1999;24:271 – 5.

**53.** Wang H, Liu D, Wang Y, Qin J, Elledge SJ. Pds1 phosphorylation in response to DNA damage is essential for its DNA damage checkpoint function. Genes Dev 2001;15:1361 – 72.

**54.** Sanchez Y, Bachant J, Wang H, et al. Control of the DNA damage checkpoint by chk1 and rad53 protein kinases through distinct mechanisms. Science 1999;286:1166 – 71.

**55.** Agarwal R, Tang Z, Yu H, Cohen-Fix O. Two distinct pathways for inhibiting pds1 ubiquitination in response to DNA damage. J Biol Chem 2003;278:45027 – 33.

**56.** Clerici M, Baldo V, Mantiero D, Lottersberger F, Lucchini G, Longhese MP. A Tel1/MRX-dependent checkpoint inhibits the metaphase-to-anaphase transition after UV irradiation in the absence of Mec1. Mol Cell Biol 2004;24:10126 – 44.

**57.** Royou A, Macias H, Sullivan W. The *Drosophila* Grp/Chk1 DNA damage checkpoint controls entry into anaphase. Curr Biol 2005; 15:334 – 9.

**58.** Cohen-Fix O, Koshland D. Pds1p of budding yeast has dual roles: inhibition of anaphase initiation and regulation of mitotic exit. Genes Dev 1999;13:1950 – 9.

**59.** Sun X, Guo T, He J, et al. Determination of the concentration of diallyl trisulfide in rat whole blood using gas chromatography with electron-capture detection and identification of its major metabolite with gas chromatography mass spectrometry. Yakugaku Zasshi 2006;126: 521 – 7.

**60.** Li H, Li HQ, Wang Y, et al. An intervention study to prevent gastric cancer by micro-selenium and large dose of allitridum. Chin Med J (Engl) 2004;117:1155 – 60.

AACR American Association for Cancer Research

Molecular Cancer Therapeutics

# Activation of a novel ataxia-telangiectasia mutated and Rad3 related/checkpoint kinase 1 –dependent prometaphase checkpoint in cancer cells by diallyl trisulfide, a promising cancer chemopreventive constituent of processed garlic

Anna Herman-Antosiewicz, Silvia D. Stan, Eun-Ryeong Hahm, et al.

*Mol Cancer Ther* 2007;6:1249-1261. Published OnlineFirst April 3, 2007.